

Numerical modeling of Hydro-Mechanical fracture behavior

C.Guiducci, F. Collin, J.P. Radu, A. Pellegrino, R. Charlier

Eni-Agip Division-Italy
Department GeomaC University of Liège,
Department GeomaC University of Liège,
Eni-Agip Division-Italy
Department GeomaC University of Liège.

A numerical approach for modeling coupled Hydro-Mechanical fracture behavior in 2D is presented in this paper. This approach accounts for the strong dependence of the flow characteristics on fracture apertures and offers an anisotropic description of the flow propagation in the fracture. An interface finite element and a constitutive model are developed. In order to validate the applicability of the model to general geomechanic problems, 2D simulations were performed. Results show the good application of the mathematical model and the fundamental hydraulic role played by the fractures.

In diesem Beitrag wird ein Stoffgesetz vorgeschlagen um hydromechanisches Kluftverhalten numerisch zu modellieren. Dieser Vorgang nimmt die starke Abhängigkeit der Fließeigenschaften von der Kluftöffnung mit in Betracht. Ein Interfaceelement und ein Stoffgesetz wurden entwickelt. Zum Validieren der Anwendbarkeit dieses Modells wurden 2D Simulationen durchgeführt. Ergebnisse haben gezeigt dass das mathematische Modell anwendbar ist und dass Klüfte eine fundamentale hydraulische Rolle spielen.

Une approche numérique pour la modélisation du comportement couplé hydro-mécanique des fractures en 2D est présentée dans ce papier. Cette approche prend en compte la forte dépendance des caractéristiques du flux de fluide sur les ouvertures des fractures et présente une description anisotrope de la propagation du flux dans la fracture. Un élément fini d'interface et un modèle constitutif sont développés. Dans le but de valider l'applicabilité du modèle à des problèmes généraux de géomécanique, des simulations 2D ont été réalisées. Les résultats montrent la bonne application du modèle mathématique et le rôle hydraulique fondamental joué par les fractures.

Introduction

Fractured oil reservoirs in petroleum engineering represent since several years an area of study of great interest concerning the production/injection estimation. Since lots of phenomena occur at different scales a global evaluation of the reservoir exploitation field gives up in complexity. In particular, an important problem is represented by the possible effect on productivity due to changes in hydraulic conductivity of the main fractures. Then, the description of single fractures behavior from a geological and a geomechanical point of view represents a subject of central importance.

Lots of studies have been performed during the last years, concerning the behavior of rock fractures; experimental investigations (Barton 1976, Bandis *et al.* 1981, Gentier 1996) together with modeling works (Goodman *et al.* 1968, Barton *et al.* 1985, Boulon *et al.* 1993) were coupled together with the purpose to offer a general description of fracture behavior from both the hydraulic and the mechanical point of view.

This paper presents a constitutive model (Bart 200), which coupled together these two aspects. The coupling between the hydraulic and the mechanical phenomena is realized

combining the cubic law with a non-linear deformation function (hyperbolic) (Goodman *et al.* 1972, Bandis *et al.* 1983) to describe the stress-closure/opening curves of the fractures. The coupling behavior under tangential effective stresses is taken into account through the simple Mohr Coulomb linear relation.

From a numerical point of view, fracture modeling is realized through a developed interface contact element implemented in Lagamine finite element code.

Through some 2D numerical simulations the validation of the constitutive model applied to the numerical interface element has been performed. Simulations were developed reproducing a schematized reservoir where a horizontal fracture was placed.

Results show the good application of the model in a simple fractured reservoir context and the fundamental hydraulic role played by the fracture. Comparisons with results obtained from a non coupled model point out the importance to consider the behavior of the fracture as coupled.

Fracture constitutive model

As shown by through literature one main point in modeling the behavior of a rock fracture lies on the description of the discontinuity itself. One of the greatest problems in reproducing its behavior depends on its complex morphology that does not permit to take directly into account clear parameter values. It is however known how strongly the geometric properties are related to the mechanical and hydraulic behavior and then to the global behavior of fractured rock masses. In the following, mechanical and hydraulic laws for fracture behavior are introduced and coupled together in order to achieve modeling of hydro-mechanical fracture behavior subjected to normal stress.

Mechanical formulation of the model

Extended experimental studies (Bandis *et al.* 1983) on natural rock fractures have shown that the relation between increasing normal stress σ_n and the normal displacement u_n is a non-linear curve resembling to a hyperbola (Figure 1).

The non-linearity is mainly due to the discontinuity stiffness evolution. Starting from a small initial value, the discontinuity stiffness increases toward the K_n value of the intact rock (K_r). In particular, experimental curves show a rapid increase of the normal discontinuity stiffness K_n (σ_n - u_n slope) with the increasing stress.

From a physical point of view this non-linear behavior can be explained from the progressive mobilization of the fracture asperities when normal loads are applied. The normal stiffness of the fracture depends on the mechanical properties of the rock and on the physical properties of the infilling material, if present, but more over on the configuration of the asperities: their number, area and relative position. At the beginning, starting from low stresses applied on the fracture, only few of its points get in contact and the deformations relative to small imposed stresses are important. Progressive applied stresses and consequently progressive fracture closure get more and more asperities in contact, displacements become then smaller until the fracture behavior can be compared to that one of the intact rock for a well-determined applied load. At this contact scenario, fracture behavior is achieving an asymptote that corresponds to the maximal fracture mechanical closure (V_m).

The mechanical model is expressed in terms of the following equation (Bart 2000):

$$\Delta\sigma_n' = \frac{K_{ni}D_0}{\left(1 + \frac{\Delta V}{D_0}\right)^\gamma} \Delta V \quad (1)$$

where:

- K_{ni} is the normal initial stiffness of the fracture;
- D_0 is the asymptotical fracture opening, related to the fracture when stresses equal to zero are applied;
- γ is an empirical coefficient variable between 2 and 6, it's value is increasing with the fracture roughness.

The K_{ni} parameter can be obtained as the initial slope of the hyperbola of Fig.1., its value can be estimated from the

rock matrix stiffness. For γ parameter Bandis *et al.* (1983) proposed a value 2 to give a correct description of the mechanical behavior of the fracture.

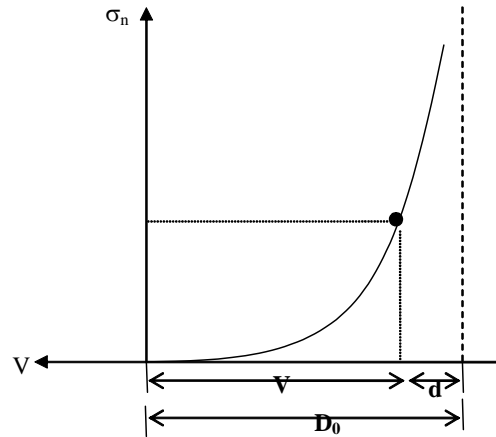


Figure 1. Example of normal stress-closure curve

Hydraulic formulation of the model

Concerning the flow behavior in fractures, parallel and orthogonal directions of fluid propagation respect to the fracture have to be considered. Flow in the two directions shows different behavior, the model takes into account the anisotropy by the definition of a transverse transmissivity T_t and of a longitudinal permeability k_l of the fracture.

So, if the fracture longitudinal permeability k_l is not nil, under the simplest hypothesis of laminar flow along smooth parallel plates, cubic law is representing the longitudinal fluid way of propagation along the fracture (Gangi 1978, Tsang and Witherspoon 1981, Schrauf and Evans 1986):

$$f_l = -\frac{d^3}{12\mu_f} (\nabla p_f + \rho_f g \nabla z) \rho_f \quad (2)$$

where the volume flow rate f_l varies as the cube of separation between the two plates d ; μ_f is the fluid viscosity; Δp_f is the fluid pressure gradient along the fracture and ρ_f is the fluid density. In this case the longitudinal permeability of the fracture is given by:

$$k_l = \frac{d^2 \rho_f g}{12\mu_f} \quad (3)$$

Dealing with the horizontal propagation of the flow into a fracture, according with the definition of a transversal transmissivity T_t , as:

$$T_t = \frac{\rho g d^3}{12\mu_f} \quad (4)$$

two different fluid flows f_{t1} and f_{t2} can be described from the following relations:

$$f_{t1} = T_t(p_f^F - p_f^I) \quad (5)$$

$$f_{t2} = T_t(p_f^I - p_f^S) \quad (6)$$

where p_f^F , p_f^S and p_f^I are respectively the pressure related to the two boundaries rock interface and to the interface element (Figure 4).

Hydro-mechanical formulation of the coupled model

The coupled model (Bart 2000) is summarized by the equations (1), (2), (5), (6) and by:

Terzaghi postulate

$$\Delta \sigma_n = \Delta \sigma'_n + \Delta p \quad (7)$$

aperture relation

$$d - V = D_0 \quad (8)$$

Interface finite element

To deal with the schematization of a general rock discontinuity the numerical approach of the finite element model was chosen. Between the various existing finite element codes, LAGAMINE was implemented in this work. LAGAMINE is a finite element code born in 1983 to simulate groove lamination and then developed in geomechanics to solve, between the others, problems bounded to soil and rock mechanics and to the hydraulic of fluids in porous media.

Obviously, to represent a rock discontinuity in LAGAMINE finite element code the presence of a special finite element is required, this is called interface finite element. So, an interface finite element has been developed with the related and adapted constitutive laws to simulate the presence of discontinuities in porous media. In particular, the interface element is represented by two interface isoparametric elements that are compatible with the solid finite elements forming the boundaries. The discontinuity behavior is, then, in LAGAMINE represented through the contact of this two bodies considered deformable in the geomechanics context.

General concept of contact problem

Consider two deformable solids (or domains) Ω^U and Ω^D with boundaries $\partial\Omega^U$ and $\partial\Omega^D$ (see Figure 2). They are contacting through boundaries $\mathcal{A}\Omega_C^U$ and $\mathcal{A}\Omega_C^D$.

At any point S of the contact surface, a local triad (e_1, e_2, e_3) can be defined for each solid as indicated on Figure 2. The e_1 axis is normal to the contact whereas the e_2 and e_3 axes are tangent. In this local referential, for a plane or axis-symmetrical problem, the stress tensor in each solid reduces to a contact stress vector $\underline{\sigma}_C$ defined by two components :

$$\underline{\sigma}_C = \begin{bmatrix} \sigma_1 \\ \sigma_2 \end{bmatrix} = \begin{bmatrix} -p \\ \tau \end{bmatrix} \quad (9)$$

where p is the pressure and τ the shear stress.

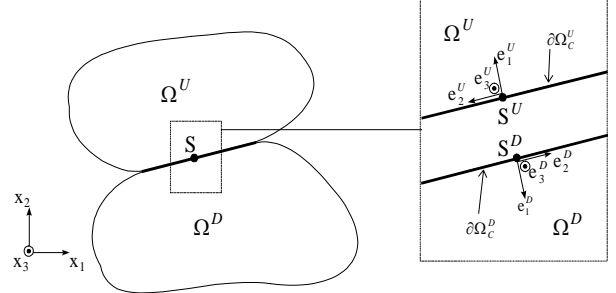


Figure 2 Contact between two deformable solids.

As this stress vector is defined in a local referential attached to a solid, it is independent of rigid body rotation, i.e. objective (Charlier & Cescotto 1988). The perfectly sticking contact condition is enforced numerically using the classical penalty method which allows a small relative velocity between points S^U and S^D , i.e. a small penetration of the two solids and a relative sliding between them.

The contact stress vector $\underline{\sigma}_C$ is associated with the relative displacement velocity $\dot{\underline{e}}_C$ (through the interface mechanical constitutive law) defined as the time derivative of the distance vector \underline{u} between $\mathcal{A}\Omega_C^U$ and $\mathcal{A}\Omega_C^D$ (see Figure 3) :

$$\dot{\underline{e}}_C = \frac{d\underline{u}}{dt} = \underline{R} \left(\frac{d\underline{x}^D - d\underline{x}^U}{dt} \right) + \frac{d\underline{R}}{dt} (\underline{x}^D - \underline{x}^U) \quad (10)$$

where the objective distance vector \underline{u} is given by

$$\underline{u} = \underline{R} (\underline{x}^D - \underline{x}^U) \quad (11)$$

and where \underline{R} represents the rotation matrix (Charlier & Cescotto 1988) between the triad (x_1, x_2, x_3) and (e_1, e_2, e_3) . Note that through the second term of equation (10), the relative velocity of the surfaces is function of the rotation rate of the local triad, which preserves objectivity.

The contact side of each body Ω^U and Ω^D can be discretised with interface isoparametric elements which are compatible with the solid finite elements used to discretise the corresponding body (Figure 3). The frictional interface elements used here are based on mixed variational (Cescotto & Charlier 1993): contact stresses are computed at contact element integration points whereas displacements of the solid boundary are computed at nodal points. This formulation leads to a smoother contact condition than the one based on nodal contact conditions.

The contact condition is simply obtained locally from geometrical computation of the distance λ_C between the two contact interfaces $\mathcal{A}\Omega_C^U$ and $\mathcal{A}\Omega_C^D$ with $\lambda_C = \underline{u} \cdot \underline{e}_1$:

- $\lambda_c < 0$ \rightarrow no contact (see Figure 3)
- $\lambda_c \geq 0$ \rightarrow there is contact.

Computation of λ_c requires choosing temporarily a reference side, for instance $\partial\Omega_C^U$. Consider an interface element U belonging to $\partial\Omega_C^U$ and an interface element D belonging to $\partial\Omega_C^D$. In this case, λ_c^U is computed between an integration point of element U (point D in Figure 3) and the intersection of the normal to this integration point with element D (point C in Figure 3).

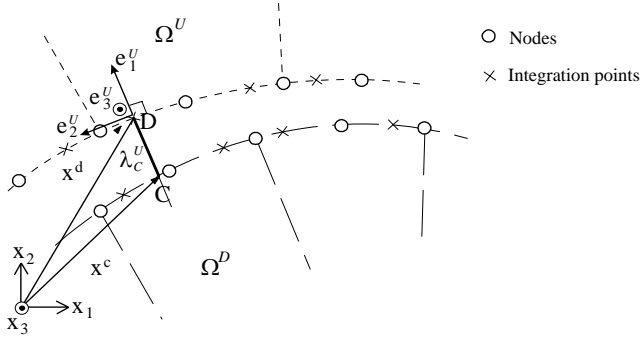


Figure 3. Parabolic interface finite elements ($\lambda_c < 0$, i.e. no contact).

For more details see (Habraken & Cescotto 1996).

Particular description of the interface element

A 2-D large strain finite element has been implemented in the LAGAMINE code. It is an isoparametric element (see Figure 4), with 2 (linear) or 3 (parabolic) nodes describing the interface element side, with 3 degrees of freedom (d.o.f) per node (2 mechanical displacements u and v , and the fluid pressure on the structure side p_f^S). To describe the seepage flow inside the interface, 2 or 3 further nodes are added with only 1 d.o.f. per node, the fluid pressure inside the interface p_f^I ; these nodes are thus the same co-ordinates that the corresponding nodes on the interface element. Of course, 2 or 3 nodes define the foundation side, with also 3 d.o.f per node (u , v , and the fluid pressure on the foundation side p_f^F).

With that element formulation, the equivalent nodal forces and the stiffness matrix in the Newton-Raphson sense will have, for a parabolic element, the following forms respectively given in (12) and (13):

$$\underline{F}^T = \left(\langle \underline{F}_S \rangle_{1 \times 9} \quad \langle \underline{F}_I \rangle_{1 \times 3} \quad \langle \underline{F}_F \rangle_{1 \times 9} \right)^T \quad (12)$$

$$\underline{K} = \begin{bmatrix} \left[\underline{K}_{SS} \right]_{9 \times 9} & \left[\underline{K}_{SI} \right]_{9 \times 3} & \left[\underline{K}_{SF} \right]_{9 \times 9} \\ \left[\underline{K}_{IS} \right]_{3 \times 9} & \left[\underline{K}_{II} \right]_{3 \times 3} & \left[\underline{K}_{IF} \right]_{3 \times 9} \\ \left[\underline{K}_{FS} \right]_{9 \times 9} & \left[\underline{K}_{FI} \right]_{9 \times 3} & \left[\underline{K}_{FF} \right]_{9 \times 9} \end{bmatrix} \quad (13)$$

where the indexes S, I and F respectively refer to the solid side, the interior interface and the foundation side.

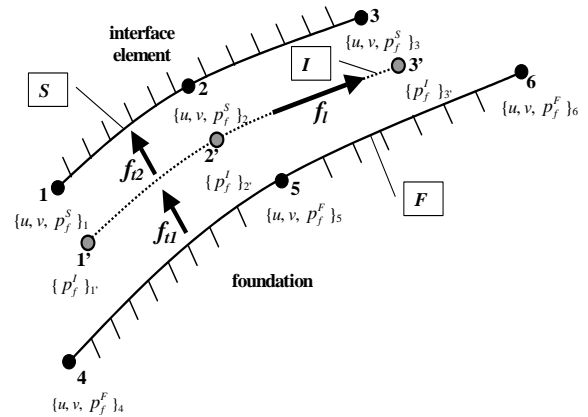


Figure 4 : Description of a 2D parabolic interface element.

Application

Boundary and initial conditions

Using the presented interface element some applications were developed. In particular a fluid depletion of a reservoir interested by a vertical well and by an horizontal fracture is modeled (Figure 5). For simplicity the fluid in the reservoir is considered to be water and the rock matrix is chalk.

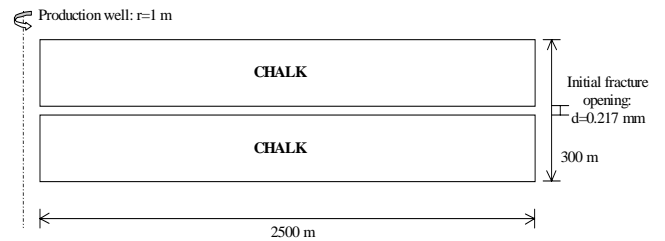


Figure 5 : Sketch of the reservoir

The reservoir is modeled in plane strain conditions the dimension being 2500 m of length by 300 m of height. The initial fracture opening value is ≈ 0.2 mm.

The initial stress field is obtained, neglecting gravity effect, from an applied 62 MPa overburden load and a 62 MPa horizontal stress imposed on the well boundary. Initial fluid pressure of the reservoir is 48.7 MPa.

A production phase was modeled starting from those initial conditions. A first step of 15 MPa fluid pressure decrease is applied for 7.5 years at the well boundary. A following second step lasting 12.5 years is perceived maintaining fluid pressure constant (Figure 6).

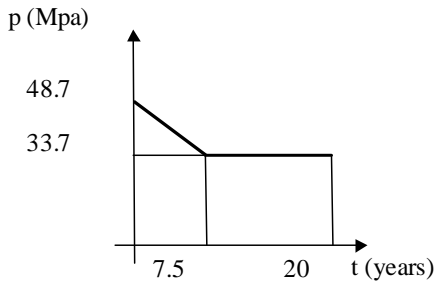


Figure 6. Production scheme

Results

Results regarding fluid pressure variation and fluid flow in the fracture are presented in the Figure 7, 8. The curves are related to the pressure and flow evolution after 7.5 and 20 years of simulation.

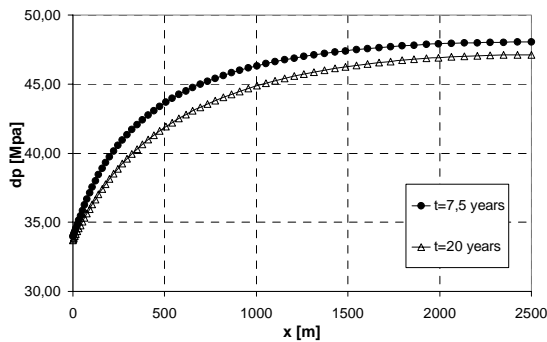


Figure 7. Fluid pressure variation along the fracture after 7.5 and 20 years of simulation.

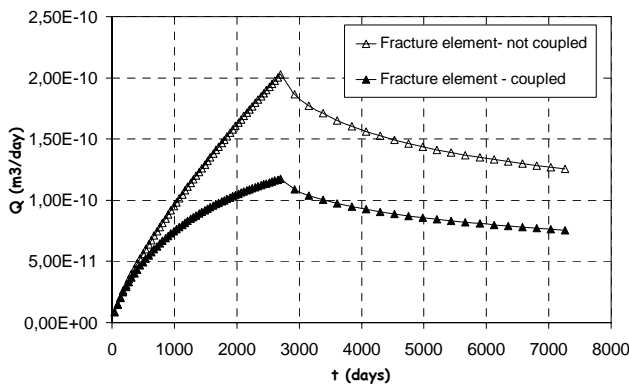


Figure 8. Flow rate trend comparison using a coupled and a non-coupled fracture model.

The important hydraulic role of the fracture is underlined through the flow rate evolution results (Figure 9). The biggest flow rate outgoing from the well boundary is due to the fracture contribution. After 7.5 years of depletion a fracture flow rate maximum is reached while after, keeping pressure constant for the following 12.5 years of simulation, a small decrease is observed. It is also observed (Figure 9) that the contributions related to the average of the flow rate outgoing from the two rock matrix to the well are coincident and negligible compared to the flow rate associated to the fracture.

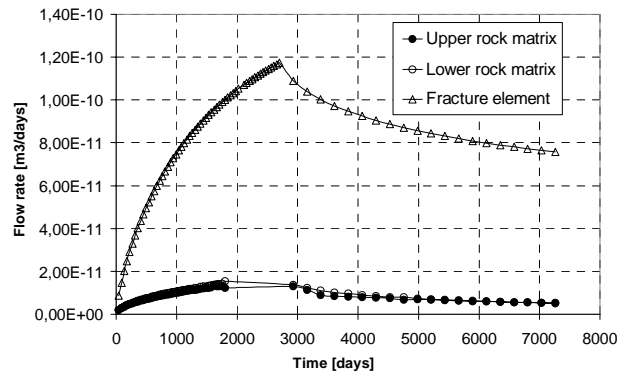


Figure 9. Outgoing flow rate variation with time increasing

Fracture coupled behavior is then put in evidence from the following results. Due to the observed fracture fluid pressure decrease, progressive fracture closure is achieved during the calculation. After 7,5 and 20 years of production simulation Figure 10 shows that in the well nearby zone a 50% reduction of the initial fracture opening is achieved, the perturbation fading with the distance from the well in agree with pressure variation trend.

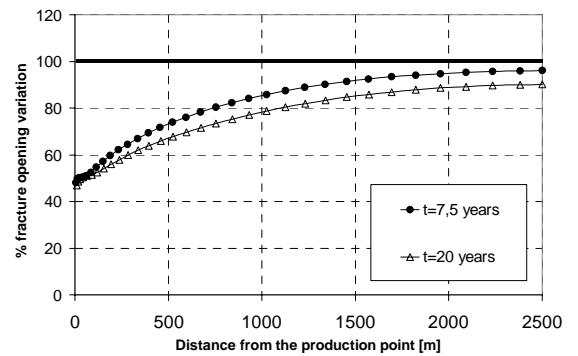


Figure 10. Fracture opening variation after 7.5 and 20 years of simulation.

As shown in Figure 10. the model succeeds in the representation of fracture hydro-mechanical behavior bounding pressure variation to fracture deformation. The importance of a good fracture description is underlined by comparisons between simulations performed by the presented fracture coupled model and a non-coupled fracture model where opening fracture is maintained constant during all the simulation time.

Comparisons

Two different fracture models were applied for the description of the same reservoir production phase. In particular, results from the precedent computation are compared with those ones obtained from the application of a non-coupled fracture model on the same reservoir schematization using the same initial and boundary conditions. From the comparisons appears that the fracture closure variation described by the coupled model heavily influences all the hydraulic parameters. So, comparisons with the non coupled model show that the progressive fracture closure is responsible of: 1) a slower fluid pressure decrease along the fracture (Figure 11); and a lower fluid

flow value along all the fracture; 2) a smaller quantity of flow rate outgoing from the fracture to the well boundary (Figure 12).

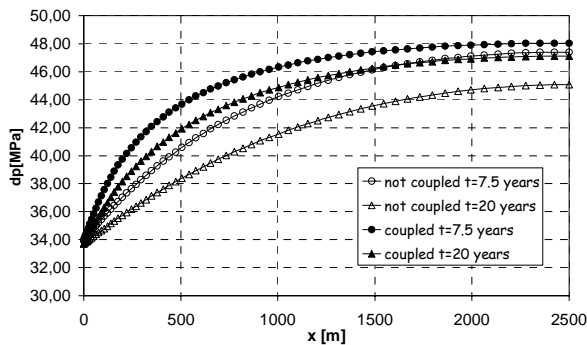


Figure 11. Fluid pressure variation comparison between coupled and non-coupled fracture model

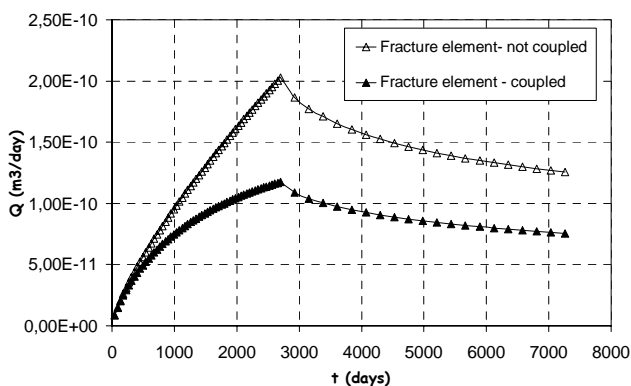


Figure 12. Flow rate trend comparison using a coupled and a non-coupled fracture model.

Conclusions

A coupled fracture model was developed in this paper to predict the influence of the hydro-mechanical fracture behavior in the oil reservoir depletion. It combines the cubic law with a non-linear deformation function (hyperbolic) suggested to describe the stress-closure/opening curves of the joints.

The model was implemented in the finite element code LAGAMINE in order to be validated. An interface finite element has also been developed in the code to be able to reproduce the fracture by a numerical point of view. The anisotropy of the fluid propagation is through this element respected.

Simulations on fracture behavior are developed around a simple reservoir geometry. Results point out the important hydraulic role played, in a reservoir, by fractures. Comparisons between the presented coupled model and a non-coupled model show relative big different in the fracture behavior description. In particular, the description offered by taking into account the coupling between hydraulic and mechanical aspects is more complete and innovative in contrast with the actual tendency to consider

fractures influence on the reservoir only from an hydraulic point of view.

References

- BANDIS, S., LUMSDEN, A.C. and BARTON, N. Experimental studies of scale effects on the shear behavior of rock joints. *Int. Jour. Of Rock Mechanics and mining Science & Geomech. Abstr.* Vol. 18 (1), pp. 1-21, 1981.
- BANDIS, S., LUMSDEN, A.C. and BARTON, N. Fundamentals of rock joints deformation. *Int. Jour. Of Rock Mechanics and mining Science & Geomech. Abstr.* Vol. 20(6), pp. 249-68, 1983.
- BART, M. Contribution à la modélisation du comportement hydromécanique des massifs rocheux avec fracture. Ph. D. Thesis, Univ. des Sciences et Technologies de Lille, 2000.
- BARTON, N. CHOUBEY, V. The shear strength of rock joints in theory and practice. *Rock Mechanics and Rock Engineering.* Vol. 10, pp. 1-54, 1976.
- BARTON, N. BANDIS, S. and BAKHTAR, K. Strength deformation and conductivity coupling of rock joints. *Int. Jour. Of Rock Mechanics and mining Science & Geomech. Abstr.* Vol. 22(3), pp. 121-140, 1985.
- CESCOTTO, S. CHARLIER, R. Frictional contact finite elements based on mixed variational principles. *Int. JI. For Numerical Methods in Engineering,* Vol. 36, pp. 1681-1701, 1993.
- CHARLIER, R. CESCOTTO, S. Modélisation du phénomène de contact unilatéral avec frottement dans un contexte de grandes déformations. *Jl. Of Theoretical and Applied Mechanics (special issue, supplement),* Vol. 7(1), 1988.
- GANGI, A. F. Variation of a whole and fractured porous rock permeability with confining pressure. *Int. J. Rock Mech. Min. Sci. and Geomech. Abstr.,* Vol 15 pp. 246-257, 1978.
- GENTIER, S., PETITJEAN, C., RISS J., ARCHAMBAULT, G., Hydromechanical behavior of a natural joint under shearing, *Rock Mechanics,* p. 1201-1208, 1996.
- GOODMAN, R. TAYLOR, R. and BREKKE, T. A model for the mechanics of jointed rock. *J. Soil Mech. Fdns Div., Proc. Am. Soc. civ. Engr,* N° 94, pp. 637-659, 1968.
- GOODMAN, R. DEBOIS, J. Duplication of dilatancy in analysis of jointed rocks. *Journal of the soil mechanics and foundations division, ASCE,* Vol. 98, SM 4 pp. 399-422, 1972.
- HABRAKEN, A.M., and CESCOTTO, S. Contact between deformable solids. The fully coupled approach. *Jl. For Mathematical and Computer Modeling (special issue: Recent advances in contact and impact mechanics),* 1996.
- SCHRAUF, T. W. and EVANS, D. Laboratory studies of gas flow through a single natural fracture. *Water Resour. Res.,* 22, 1038-1050, 1986.
- TSANG, Y. W., WITHERSPOON P. A., Hydromechanical behavior of a deformable rock fracture subject to normal stress. *J. Geophys. Res.* 86, 9287-9298, 1981.